

Van Roosbroeck's equations with topological terms: The case of Weyl semimetals

Pierre-Antoine Graham, Simon Bertrand, Michaël Bédard , Robin Durand , and Ion Garate
*Département de Physique, Institut Quantique and Regroupement Québécois sur les Matériaux de Pointe,
 Université de Sherbrooke, Sherbrooke, Québec, Canada J1K 2R1*



(Received 10 August 2022; revised 2 June 2023; accepted 26 June 2023; published 5 July 2023)

Van Roosbroeck's equations constitute a versatile tool to determine the dynamics of electrons under time- and space-dependent perturbations. Extensively utilized in ordinary semiconductors, their potential to model devices made from topological materials remains untapped. Here, we adapt van Roosbroeck's equations to theoretically study the bulk response of a Weyl semimetal to an ultrafast and spatially localized light pulse in the presence of a quantizing magnetic field. We predict a transient oscillatory photovoltage that originates from the chiral anomaly. The oscillations take place at the plasma frequency (THz range) and are damped by intervalley scattering and dielectric relaxation. Our results illustrate the ability of van Roosbroeck's equations to unveil the interplay between electronic band topology and fast carrier dynamics in microelectronic devices.

DOI: [10.1103/PhysRevB.108.024301](https://doi.org/10.1103/PhysRevB.108.024301)

I. INTRODUCTION

Van Roosbroeck's (VR) system of equations [1] comprises the drift-diffusion and continuity equations for electric charge carriers with the Poisson equation for the electric field. These equations have been key for the understanding and development of landmark devices, such as transistors, solar cells, and photodiodes. As such, numerous studies and monographs have been published about the VR equations and their solutions (see, e.g., Refs. [2–7]). Modern commercial software packages [8] are also equipped to solve the VR equations in a variety of realistic device geometries. Yet, the aforementioned works and software have been tailored to topologically trivial materials.

It is now known that a large fraction of solids host topologically nontrivial electrons [9–11]. Thus, there is a marked interest toward creating devices that will exploit the topological properties of matter [12,13]. Remarkably, although drift-diffusion equations have been used to predict novel electrical transport properties in certain topological materials under restricted (e.g., static) conditions [14], full-fledged VR equations remain vastly underexploited therein. Little is known about fundamental changes that could emerge in the solutions of those equations when electrons have a nontrivial band topology. If topological microelectronic devices are to become technological reality, then such a gap of knowledge must be filled. The objective of our paper is to make progress in this direction and to show that VR equations, appropriately adapted to account for nontrivial electronic topology, can unveil new physical effects in topological devices of potential technological interest.

The family of topological materials being large and diverse, we are inclined to make a choice for the purposes of the present study. The material that we focus on is a Weyl semimetal (WSM), where pairs of nondegenerate electronic bands cross at isolated points in the Brillouin zone [15]. These points, called Weyl nodes, are sources or sinks of Berry curvature and have a chirality index $\chi = \pm 1$, which is a topological invariant of the electronic band structure.

Recently, the investigation and control of WSM using ultrafast light has emerged as a frontier of fundamental and applied research [16,17]. On the one hand, the influence of the Berry curvature in photodetection and nonlinear optics has been highlighted [12,18–20]. On the other hand, experiments [21–23] have measured the light-induced chiral anomaly, a topological property whereby collinear electric and magnetic fields induce a transfer of electrons between Weyl nodes of opposite chirality [24].

In this paper, we investigate the interplay between electronic band topology and transient carrier dynamics in a WSM irradiated by a spatially inhomogeneous light pulse (Fig. 1), using a new approach. We begin by writing VR equations for a WSM placed under a strong magnetic field and subject to a light pulse (Sec. II), with adjustments to accommodate for the nontrivial electronic band topology. We follow in Secs. III and IV by linearizing and solving the preceding VR equations. Our strategy of solution is to posit simple but physically justified boundary conditions, and then to take advantage of them by integrating the VR equations over the system's length. This approach enables us to gain analytical insight for a physical quantity of interest, namely the photovoltage. We thus find a transient photovoltage that oscillates at the plasma frequency. The oscillations originate from the chiral anomaly and are driven by an internal electric field that results from the spatial separation between photoexcited electrons and holes. Unlike in Refs. [21–23], the effect of the chiral anomaly is present even when the electric field of light is perpendicular to the static magnetic field. The main text of the paper ends with some discussion (Sec. V) and conclusions (Sec. VI). The six Appendices contain technical aspects that allow us to reproduce the main results of the paper.

II. BASIC EQUATIONS

In this section, we adapt the VR equations to a bulk WSM with two nodes. The nodes of opposite chirality are related by symmetry and the energy dispersion is untilted. A strong static

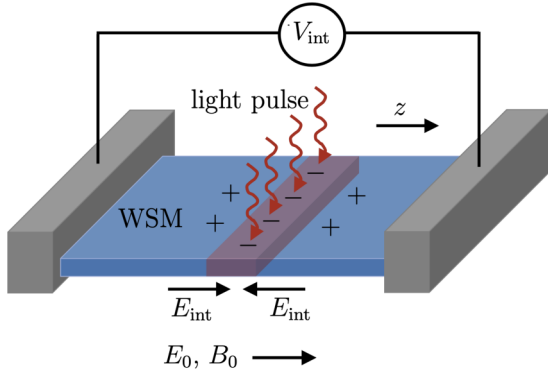


FIG. 1. A Weyl semimetal film (blue) is placed between two contacts (gray). Initially, the WSM is subjected to an electric field $E_0\hat{z}$ and a magnetic field $B_0\hat{z}$, both uniform and static. Then, a finite region of length dz (red) is illuminated with a light pulse of duration dt . Photoexcited electrons ($-$) and holes ($+$) drift and diffuse away unequally from the illuminated region, giving rise to a local charge accumulation and a concomitant electric field E_{int} . The line integral of E_{int} between the contacts yields a transient photovoltage V_{int} that oscillates at the plasma frequency due to the chiral anomaly.

and uniform magnetic field $\mathbf{B}_0 = B_0\hat{z}$ is applied, so that the equilibrium Fermi energy ϵ_F intersects solely with the chiral ($n = 0$) Landau levels (Fig. 2). It is in this regime that the effect of chiral anomaly in VR equations is most pronounced. In Appendix F, we present the corresponding theory for a weak B_0 .

We restrict our analysis to the electronic dynamics in the $n = 0$ and $n = 1$ Landau levels. We assume that (i) all the other bands are far enough from ϵ_F , and their electronic populations unchanged by the light pulse; (ii) the occupation of the $n = 1$ bands in thermal equilibrium is small (low

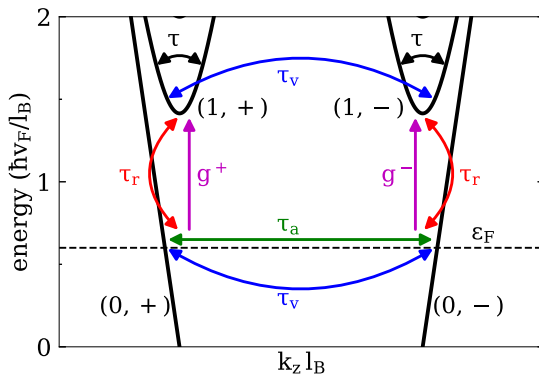


FIG. 2. Low-energy Landau bands (n, χ), with $n = 0, 1$ and $\chi = \pm 1$. The $n = 0$ bands are unidirectional, due to the nontrivial electronic band topology. The magnetic length is l_B and k_z stands for the electronic wave vector component parallel to the static magnetic field. The equilibrium Fermi energy is ϵ_F (dashed lines). Other important parameters are (i) the intraband relaxation time τ in the $n = 1$ bands, (ii) the intervalley relaxation time τ_v , (iii) the intervalley electron-hole recombination time τ_r , (iv) the characteristic time τ_a for intervalley charge transfer along chiral Landau levels due to the chiral anomaly, and (v) the optical generation rates g^\pm . In the main text, we adopt the hierarchy $\tau < \tau_a \lesssim \tau_r \ll \tau_v$.

temperature); (iii) the light pulse is uniform across the film thickness and width, but nonuniform along the film length z (Fig. 1). Assumption (iii) justifies the use of one-dimensional VR equations, which we enumerate and discuss next.

In the drift-diffusion approximation, the charge current density along z for the band $(1, \chi)$ is

$$j_1^\chi = q\mu_1\rho_1^\chi E + qD_1\partial_z\rho_1^\chi, \quad (1)$$

where ρ_1^χ is the electron number density in band $(1, \chi)$, q is the absolute value of the electron's charge ($q > 0$), E is the z component of the total electric field (including a static and uniform electric field E_0 , the electric field of light E_{light} , and an internal electric field E_{int} discussed below), $\mu_1 = q\tau/m^* = q|v|\tau l_B/(\sqrt{2}\hbar)$ is the mobility of electrons in the $n = 1$ band in the effective mass (m^*) approximation, $|v|$ is the Fermi velocity, τ is the intraband scattering time in band $(1, \chi)$, $l_B = \sqrt{\hbar/(q|B_0|)}$ is the magnetic length and $D_1 = v^2\tau$ is the diffusion coefficient. Hereafter, τ is assumed to be the shortest of all characteristic times in the problem, thereby justifying time-locality in Eq. (1).

The charge current density along z in band $(0, \chi)$ is

$$j_0^\chi = \chi qv\rho_0^\chi, \quad (2)$$

where $v = |v|\text{sgn}(B_0)$ is the (constant) slope of band $(0, -)$ and ρ_0^χ is the electron number density therein. The reason why Eq. (2) looks different from Eq. (1) is that the motion of electrons in a chiral Landau level is one-way. Accordingly, one cannot write the current in a *single* chiral Landau level as a sum of drift and diffusion currents. This is an example of how electronic band topology requires adjusting the VR equations away from their traditional form. It turns out that the total current in the chiral Landau levels, $j_0^+ + j_0^-$, can be written in terms of drift and diffusion currents if time variations of the current are slow on the scale of the intervalley relaxation time τ_v (see Appendix A). Since we are interested in the dynamics that is faster than τ_v , $j_0^+ + j_0^-$ is not simply a sum of drift and diffusion currents.

The charge continuity equation for band (n, χ) reads

$$\partial_z j_n^\chi - q\partial_t \rho_n^\chi = qR_n^\chi + qG_n^\chi - \chi \frac{q^3 E B_0}{4\pi^2 \hbar^2} \delta_{n,0}, \quad (3)$$

where δ is a Kronecker delta,

$$G_0^\chi = -G_1^\chi \equiv g^\chi(z, t)/2 \quad (4)$$

is the $(0, \chi) \rightarrow (1, \chi)$ optical generation rate ($g^\chi > 0$) in units of $1/(\text{time} \times \text{volume})$,

$$R_1^\chi = \chi \frac{\rho_1^+ - \rho_1^-}{\tau_v} + \frac{\rho_1^\chi - \rho_{1,\text{eq}}^\chi}{\tau_r}, \quad (5)$$

$$R_0^\chi = \chi \frac{\rho_0^+ - \rho_0^-}{\tau_v} - \frac{\rho_0^\chi - \rho_{0,\text{eq}}^\chi}{\tau_r} \quad (6)$$

are the relaxation rates for the excess charge in the relaxation time approximation, τ_r is the intervalley electron-hole recombination time, and $\rho_{1,\text{eq}}^\chi$ is the equilibrium electron density in band $(1, \chi)$. We have for simplicity assumed that τ_v is the same for $n = 0$ and $n = 1$. By considering all relaxation times to be constants, we focus on electron dynamics not far from equilibrium.

The second term in the right-hand side (r.h.s.) of Eq. (6) ensures the conservation of the total charge via $\sum_{n,\chi} (\partial_z j_n^\chi - q \partial_t \rho_n^\chi) = 0$. The third term in the r.h.s. of Eq. (3) is the chiral anomaly term, which in the low-temperature regime enters directly only in the continuity equation for the band intersecting the Fermi level ($n = 0$).¹ This term, absent in traditional VR equations, is another example of the adaptation required by nontrivial band topology.

In Eq. (4), g^χ is calculable from Fermi's golden rule (see Appendix B). Two properties of g^χ worth noting are that (i) $g^\chi \propto |B_0|$ due to the Landau level degeneracy, and (ii) $g^+(z, t) = g^-(z, t)$ if the light pulse preserves the symmetry relating the two Weyl nodes. The latter property fails when $E_0 \neq 0$, which breaks the $z \rightarrow -z$ symmetry. Before light illumination, Eqs. (3), (5), and (6) yield

$$\rho_0^\chi = \rho_{0,\text{eq}}^\chi + \chi \frac{q^2 \tau_v}{8\pi^2 \hbar^2} E_0 B_0 \quad \text{and} \quad \rho_1^\chi = \rho_{1,\text{eq}}^\chi, \quad (7)$$

which implies $\rho_0^+ - \rho_0^- \propto E_0 \neq 0$, as though the two Weyl nodes have different chemical potentials. If so, then $g^+ \neq g^-$ even when the light pulse preserves the crystal symmetry.

For later reference, the electric current in the absence of a light pulse is obtained from Eq. (7) and reads

$$j = \sigma_0 E_0 + q v_d (\rho_{1,\text{eq}}^+ + \rho_{1,\text{eq}}^-), \quad (8)$$

where $v_d = \mu_1 E_0$ is the drift velocity in $n = 1$ bands and

$$\sigma_0 = q^3 v B_0 \tau_v / (4\pi^2 \hbar^2) \quad (9)$$

is the dc conductivity from $n = 0$ bands.

Last, the longitudinal part of the electric field obeys the Poisson equation

$$\partial_z E = -(q/\epsilon) \sum_{n=0,1} \sum_{\chi=\pm 1} (\rho_n^\chi - \rho_{n,\text{eq}}^\chi), \quad (10)$$

where ϵ is the dielectric constant of the material and the equilibrium charge densities are assumed to be spatially uniform (homogeneous doping).

Because E_{light} is transverse and E_0 is independent of z , E in Eq. (10) equals an internal, photoinduced electric field E_{int} . Initially, photoexcited electrons and holes propagate at different speeds due to the markedly different energy dispersions of the $n = 0$ and $n = 1$ bands. Consequently, a local net charge is generated in the region where the light pulse acts, which in turn produces E_{int} . This field tends to neutralize the local charge at times exceeding the dielectric relaxation time.

Neglecting thermoelectric effects [26] for simplicity, Eqs. (1)–(6) and (10) form the complete VR system of equations for the unknowns ρ_n^χ and E . These nonlinear and coupled equations must in general be solved numerically. Nevertheless, as we show next, analytical insights about the transient optoelectronic response of WSM can be gained by linearizing the VR equations and solving them with simple boundary conditions.

¹We neglect the magnetic field of the light pulse and we likewise neglect light-induced lattice strains and their possible contributions [25] to the chiral anomaly term.

III. LINEARIZED EQUATIONS

Let us define $\Sigma_n \equiv \sum_\chi (\rho_n^\chi - \rho_{n,\text{eq}}^\chi)$ and $\Delta_n \equiv \sum_\chi \chi (\rho_n^\chi - \rho_{n,\text{eq}}^\chi)$ as the deviations of the scalar and chiral electron densities from equilibrium (respectively). For an optical pulse of modest intensity, VR equations can be linearized in Σ_n and Δ_n (see Appendix C):

$$(D_1 \partial_z^2 + v_d \partial_z - \partial_t - 1/\tau_r) \Sigma_1 = -g_s,$$

$$(D_1 \partial_z^2 + v_d \partial_z - \partial_t - 1/\tau_r - 2/\tau_v) \Delta_1 = -g_d,$$

$$v \partial_z \Delta_0 - \partial_t \Sigma_0 + \Sigma_1/\tau_r = g_s,$$

$$v \partial_z \Sigma_0 - (\partial_t + 2/\tau_v) \Delta_0 + \Delta_1/\tau_r = g_d - \epsilon E / (q v \tau_a^2),$$

$$\Sigma_0 + \Sigma_1 = -\epsilon \partial_z E_{\text{int}} / q, \quad (11)$$

where $g_s = \sum_\chi g^\chi / 2$ and $g_d = \sum_\chi \chi g^\chi / 2$ are the scalar and chiral optical generation rates (respectively), and

$$\tau_a = \sqrt{\frac{\tau_v \epsilon}{2 \sigma_0}} \quad (12)$$

is a characteristic time that emerges from the chiral anomaly term in Eq. (3). Physically, ϵ/σ_0 is the dielectric relaxation time and τ_a^{-1} is the bulk plasma frequency of chiral electrons (the zero of the zz component of the dielectric tensor) in the absence of scattering [27].

In Eq. (11), the electron dynamics in the $n = 0$ bands is affected by the dynamics in the $n = 1$ bands, but not vice versa. Also, the fourth line of Eq. (11) captures the dynamical internodal charge pumping induced by E_{light} by virtue of the chiral anomaly [21–23]. Hereafter, we assume that $E_{\text{light}} = 0$ (i.e., $\mathbf{E}_{\text{light}} \perp \mathbf{B}_0$). Even then, E_{int} drives a dynamical chiral anomaly because it is collinear to B_0 . Next, we investigate its physical consequence.

IV. TRANSIENT PHOTOVOLTAGE

Equation (11) can be solved analytically for a WSM film of length L placed between two contacts, and subject to a light pulse that has a finite extent in space and time (Fig. 1). The light pulse is centered at time $t = 0$ and the spatial region where it acts is sufficiently far from the contacts. Accordingly, the deviations of the carrier densities with respect to equilibrium vanish when $z \rightarrow \pm L/2$ (contact location) or $t \rightarrow \pm \infty$. These boundary conditions allow us to solve Eq. (11) by Fourier transform (see Appendix D). Next, we summarize the approach and the results.

We begin by recognizing that the total electric current density along z can be written as

$$J_{\text{tot}} = \sum_{n,\chi} j_n^\chi + \epsilon \partial_t E_{\text{int}}, \quad (13)$$

where the first term in the r.h.s. stands for the particle current and the second term is the displacement current. Out of these parts, the drift current produced by E_0 is static [Eq. (8)]; the remaining parts are induced by the light pulse and are therefore transients.

According to Ampère-Maxwell's law, the total electric current density must be divergenceless, which in our model amounts to $\partial_z J_{\text{tot}} = 0$ [28]. Since by construction all transient effects vanish at the contacts, it follows that J_{tot} must be

everywhere static and its value given by Eq. (8). In sum, for our boundary conditions, the light pulse has no effect on J_{tot} , as though the system were connected to a constant current source.

Contrary to the total current, the voltage drop across the system *is* influenced by the light pulse. To see this, we combine Eqs. (1), (2), (8), and (13) to get

$$\epsilon \partial_t E_{\text{int}} = -\delta j, \quad (14)$$

where

$$\delta j = qv_d \Sigma_1 + qD \partial_z \Sigma_1 + qv[\Delta_0 - \sigma_0 E_0 / (qv)] \quad (15)$$

is the particle photocurrent. In the limit $\tau_a \rightarrow 0$, Eq. (11) yields $\Sigma_0 = -\Sigma_1$ (charge neutrality for all z and t) and hence $E_{\text{int}} = 0$. By Eq. (14), δj also vanishes when $\tau_a \rightarrow 0$. This is the ambipolar transport regime [29], in which photoexcited electrons of $n = 1$ bands and photoexcited holes of $n = 0$ bands track each other locally due to electrical attraction, thereby canceling their currents. For $\tau_a \neq 0$, ambipolar transport sets in at $t \gg \tau_a$.

Integrating Eq. (14) over the length of the film with the given boundary conditions, we get

$$\epsilon \partial_t V_{\text{int}} = \delta \bar{j} = qv_d \bar{\Sigma}_1 + qv \bar{\Delta}_0 - \sigma_0 E_0 L, \quad (16)$$

where $\bar{f}(t) \equiv \int_{-L/2}^{L/2} dz f(z, t)$ and $V_{\text{int}} = -\bar{E}_{\text{int}}$ is the transient photovoltage. In Eq. (16), $\bar{\Sigma}_1$ and $\bar{\Delta}_0$ obey

$$\begin{aligned} \left(\partial_t^2 + \frac{2\partial_t}{\tau_v} + \frac{1}{\tau_a^2} \right) \bar{\Delta}_0 &= \frac{\sigma_0 E_0 L}{qv\tau_a^2} - \frac{v_d \bar{\Sigma}_1}{v\tau_a^2} + \frac{\partial_t \bar{\Delta}_1}{\tau_r} - \partial_t \bar{g}_d, \\ (\partial_t + 1/\tau_r + 2/\tau_v) \bar{\Delta}_1 &= \bar{g}_d, \\ (\partial_t + 1/\tau_r) \bar{\Sigma}_1 &= \bar{g}_s, \end{aligned} \quad (17)$$

which are obtained by a spatial integration of Eq. (11). In the first line of Eq. (17), we have used Eq. (16) to replace $\partial_t \bar{E}_{\text{int}}$.

To make further progress, we need additional information about the applied light pulse. As such, we consider $\bar{g}^x(t)$ to be Gaussian with a time width dt and an amplitude $\bar{g}_0^x / (\sqrt{2\pi} dt)$, where \bar{g}_0^x is a constant. Then, a simple analytical solution of Eq. (17) is realized in the regime $\tau_a \ll (\tau_r, \tau_v)^2$ and $t \gg dt$ (see Appendix E). Substituting that solution in Eq. (16), integrating over time and imposing $V_{\text{int}}(t \rightarrow \infty) = 0$, we get

$$V_{\text{int}}(t) \simeq \frac{q}{\epsilon} (v_d \bar{g}_{0,s} - v \bar{g}_{0,d}) \tau_a e^{-\frac{dt^2}{2\tau_a^2} - \frac{t}{\tau_v}} \sin(t/\tau_a), \quad (18)$$

where $\bar{g}_{0,s} = \sum_{\chi} \bar{g}_0^{\chi} / 2$ and $\bar{g}_{0,d} = \sum_{\chi} \chi \bar{g}_0^{\chi} / 2$. Figure 3(b) displays Eq. (18), together with the numerical solution obtained from Eqs. (16) and (17). Figure 3(a) shows the photoinduced internal electric field, calculated numerically from Eq. (11).

²The typical value of τ_a in the quantum limit is ~ 0.1 ps, which is orders of magnitude smaller than τ_v [14,21]. For τ_r , we anticipate (see Appendix B) a value $\lesssim 1$ ps. Thus, while $\tau_a \ll \tau_r$ is reasonable, $\tau_a \simeq \tau_r$ could also occur. In the latter case, the analytical expression in Eq. (18) is less accurate, but remains in semi-quantitative agreement with the numerical solution of Eq. (17).

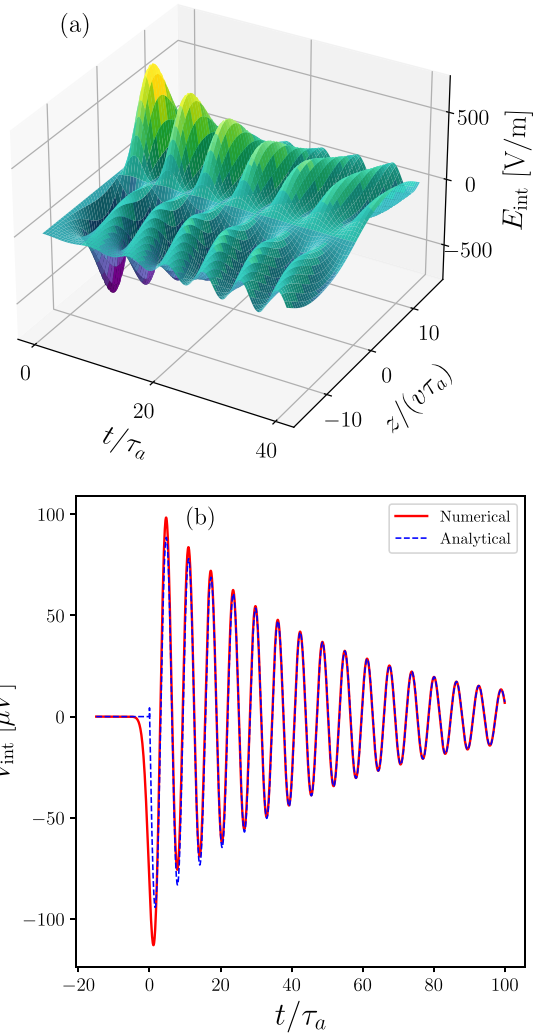


FIG. 3. (a) Longitudinal electric field induced by a Gaussian light pulse, centered at position $z = 0$ and time $t = 0$. The parameter values (see main text) are: $\tau_a = 0.25$ ps, $dt = 0$, $dz = 0.1$ μm , $\tau_r = 20\tau_a$, $\tau_v = 50\tau_a$, $v = 10^5$ m/s, $\epsilon = 30\epsilon_0$, $v_d = 0$, $\bar{g}_s = 10^{14}$ m⁻², $\bar{g}_d = 0$. In this case, $E_{\text{int}}(z) = -E_{\text{int}}(-z)$. (b) Photovoltage (line-integral of the longitudinal electric field), calculated from Eq. (17). Oscillations at the plasma frequency τ_a^{-1} stem from the chiral anomaly. The parameter values are the same as in panel (a), except that $dt = 1.5\tau_a$, $v_d = 100$ m/s and $\bar{g}_d = 0.2\bar{g}_s$. The analytical [Eq. (18)] and numerical solutions coincide when $\tau_a \ll \tau_r, \tau_v$ and $t \gg dt$.

V. DISCUSSION

Equation (18), the key result of this work, can be interpreted as follows. A light pulse induces a charge separation in the illuminated region and nearby. The resulting electric field, E_{int} , creates a neutrality-restoring current through the chiral anomaly, but it overshoots and starts plasma oscillations in the $n = 0$ bands. These oscillations are damped by intervalley scattering, which relaxes the current produced by E_{int} . If crystal symmetry is preserved, then $E_{\text{int}}(z)$ is odd in z and thus $V_{\text{int}}(t) = 0$ [see Fig. 3(a) and Appendix D]. Breaking the $z \rightarrow -z$ symmetry, by either $E_0 \neq 0$ or by the shape of the light pulse ($\bar{g}_{0,d} \neq 0$), allows for $V_{\text{int}}(t) \neq 0$. If the pulse

is slow ($dt \gg \tau_a$), then the ambipolar regime sets in while the sample is being illuminated and V_{int} is suppressed.

Although the *oscillations* in V_{int} originate from the chiral anomaly, the latter is not required to have $V_{\text{int}} \neq 0$. We can “turn off” the chiral anomaly in VR equations by taking $\tau_a \rightarrow \infty$. Experimentally, τ_a can be increased by either reducing B_0 or by rotating \mathbf{B}_0 away from z . As soon as $\tau_a > \tau_v$, the dynamics of $\overline{\Delta_0}$ in Eq. (17) becomes overdamped and hence V_{int} decays monotonically in time (see also Appendix F).

The appearance of plasma oscillations under light irradiation may seem surprising: bulk plasmons cannot be directly excited by light because they are longitudinal waves, while light waves are transverse (see, e.g., Ref. [30]). Yet, our result is enabled by an indirect mechanism: the asymmetric propagation of electrons and holes excited by light generates a *longitudinal* internal electric field, which can drive plasma oscillations. Furthermore, this mechanism is not unique to topological semimetals: photoinduced plasma oscillations have been observed in semiconductors of trivial band topology [31–33], where they have attracted much interest as a source of THz radiation. What sets WSM apart is (i) the role of band topology (tunable via \mathbf{B}_0), (ii) the ability to attain the quantum limit with modest B_0 , and (iii) the relatively long relaxation time τ_v (due to the relatively large separation in momentum space between counter-moving electrons in the $n = 0$ bands).

Let us estimate the magnitude of V_{int} . For $B_0 \simeq 5\text{T}$, $|v| \simeq 10^5$ m/s and $\epsilon = 30\epsilon_0$ (where ϵ_0 is the vacuum permittivity), we have $\tau_a \simeq 0.2$ ps. Taking $\tau \simeq 0.1$ ps, we get $\mu_1 \simeq 0.1$ m²/(Vs). Then, $E_0 \simeq 1000$ V/m gives $v_d \simeq 100$ m/s. Using Eq. (9) and $\tau_v \simeq 10$ ps, the dc current density is $\simeq 3 \times 10^7$ A/m². For a WSM film of cross section $100 \mu\text{m} \times 1 \mu\text{m}$, the dc current is modest (~ 3 mA). An optical generation rate of 10^{25} pairs/(s cm³) (in Appendix B we estimate that this rate may be attainable with an optical power of ~ 1 W), acting during a time $dt \simeq \tau_a$ within a length $dz \simeq 100 \mu\text{m}$, gives $\overline{g_{0,s}} \simeq 10^{14}$ m⁻². If $\overline{g_{0,d}} = 0$, then we arrive at $V_{\text{int}}(t) \lesssim 1 \mu\text{V}$.

There are a few strategies to increase V_{int} . First, increasing the power of the optical pulse may be possible, though nonlinear effects neglected in our theory might then need consideration. Second, the use of a *p-n* junction with a built-in electric field will render E_0 unnecessary, thereby removing the steady state electric current. Third, in a WSM with multiple pairs of nodes related by time-reversal, each of such pairs will give additive contributions to V_{int} . Fourth, in chiral topological semimetals, $\overline{g_d} \simeq \overline{g_s}$ due to the low crystal symmetry and thus V_{int} could be a factor $|v/v_d| \gg 1$ larger than in the estimate of the preceding paragraph [see also Fig. 3(b), where $\overline{g_d} \neq 0$].

VI. CONCLUSIONS

Solving Van Roosbroeck's equations for topologically non-trivial electronic bands, we have predicted photoinduced plasma oscillations in Weyl semimetals and have elucidated their relation to chiral anomaly. Our findings suggest that it may be interesting to adapt and apply VR equations to model a wide variety of topological microelectronic devices.

There are various possible open questions for further work. First, we assumed that the temperature of the system remains constant and uniform under laser irradiation. Yet, this may not

be accurate for high laser intensities. What is the influence of electronic band topology in the dynamics and spatial profile of the temperature?

Second, we assumed that the VR equations can be linearized. This requires small departures from equilibrium and therefore limits the scope of our theory. What is the effect of the topological terms in the nonlinear regime of VR equations?

Third, we considered the effect of the chiral anomaly in the VR equations for bulk electrons in a Weyl semimetal. One could study other materials, in which topological quantities should impact the solutions of VR equations.

Fourth, we considered a simple device geometry with simple boundary conditions. If topological microelectronic devices become a technological reality, then VR equations augmented with topological terms will need to be solved in more realistic settings using appropriately adapted simulation software.

ACKNOWLEDGMENTS

This work has been financially supported by the Canada First Research Excellence Fund, the CNRS-Sherbrooke International Research Laboratory on Quantum Frontiers, the Natural Sciences and Engineering Research Council of Canada (Grant No. RGPIN- 2018-05385), and the Fonds de Recherche du Québec Nature et Technologies. I.G. thanks D. Morris and T. Szkopek for helpful discussions.

APPENDIX A: DRIFT AND DIFFUSION CURRENTS FOR THE $n = 0$ LANDAU LEVEL

Combining Eqs. (2), (3), (4), and (6) of the main text, the total current in the chiral Landau level, $j_0 = j_0^+ + j_0^-$, can be rewritten as

$$j_0 + \frac{\tau_v}{2} \frac{\partial j_0}{\partial t} = \sigma_0 E + \frac{1}{2} q v^2 \tau_v \frac{\partial(\rho_0^+ + \rho_0^-)}{\partial z} - \frac{1}{4} q v \tau_v (g^+ - g^-) - q v \frac{\tau_v}{2\tau_r} (\rho_1^+ - \rho_1^-). \quad (\text{A1})$$

The first two terms in the right-hand side of this equation are the drift and diffusion currents, respectively, with a diffusion constant $D_0 = v^2 \tau_v / 2$. Note that $D_0 = \sigma_0 / [e^2 v(\epsilon_F)]$ in consistency with the Einstein relation, where the conductivity σ_0 is defined in the main text and $v(\epsilon_F)$ is the density of states at the Fermi level. The last two terms in the right-hand side of Eq. (A1) are currents that emerge due to an unequal light absorption on the two nodes. The left-hand side of the equation contains j_0 and the time-derivative of j_0 . This means that, in general, the relation between the current and the carrier density (or the electric field) is nonlocal in time. However, if the current varies slowly on the timescale of τ_v , then $j_0 \gg \tau_v \partial j_0 / \partial t$ and one arrives at the usual drift-diffusion approximation with a local-in-time relation between the current and the carrier densities (or the electric field). Since we are interested in the dynamics at timescales that are shorter than τ_v , we do not neglect the $\partial j_0 / \partial t$ term in our analysis.

APPENDIX B: FERMI GOLDEN RULE ESTIMATES FOR THE OPTICAL GENERATION RATE AND RADIATIVE RECOMBINATION TIME

In this section, we provide a numerical estimate for the optical generation rate from the $n = 0$ to the $n = 1$ Landau level, at fixed chirality χ . Then, we estimate an upper bound for the radiative recombination time (denoted τ_r is the main text) from the $n = 1$ Landau level to the $n = 0$ Landau level.

1. Fermi golden rule estimate for the optical generation rate

For the purposes of the estimate, let us first consider a monochromatic light of frequency ω , wave vector \mathbf{q} and polarization vector $\hat{\mathbf{e}}$, whose vector potential is given by

$$\mathbf{A} = \frac{A_0}{2} \hat{\mathbf{e}} [e^{i(\mathbf{q}\cdot\mathbf{r}-\omega t)} + e^{-i(\mathbf{q}\cdot\mathbf{r}-\omega t)}]. \quad (\text{B1})$$

From Fermi's golden rule [34], the generation rate [in units of $1/(\text{volume} \times \text{time})$] can be written as

$$G_0^\chi = \frac{2\pi}{\hbar} \frac{1}{2\pi l_B^2 L} \frac{1}{L} \sum_k |\langle \psi_{k\chi 1} | H_R | \psi_{k\chi 0} \rangle|^2 (f_{k\chi 0} - f_{k\chi 1}) \times \delta(E_{k\chi 1} - E_{k\chi 0} - \hbar\omega), \quad (\text{B2})$$

where l_B is the magnetic length, L is the system length along z , $|\psi_{k\chi n}\rangle$ is the electronic eigenstate for the n th Landau level of chirality χ at wave vector k along z , E_{kn} is the corresponding energy, $f_{k\chi n}$ is the Fermi-Dirac occupation factor,

$$H_R = -\frac{eA_0}{2} e^{i\mathbf{q}\cdot\mathbf{r}} \hat{\mathbf{e}} \cdot \mathbf{v} \quad (\text{B3})$$

is the light-matter coupling Hamiltonian, and \mathbf{v} is the electronic velocity operator. In Eq. (B2), we have neglected the photon wave vector in the electronic interband transitions. This is appropriate for the THz frequency light we are interested in (the energy separation between the $n = 0$ and $n = 1$ for a field of a few Tesla is in the THz regime).

For Weyl fermions, $\langle \psi_{k\chi 1} | \mathbf{v} | \psi_{k\chi 0} \rangle$ and $E_{k\chi n}$ can be obtained analytically (see, e.g., Ref. [27]). Thereafter, the integration over k in Eq. (B2) can also be carried out analytically, using the Dirac δ function. Thus, for a polarization vector along x , we get

$$G_0^\chi \simeq \frac{e^2 v A_0^2}{16\pi \hbar^2 l_B^2}, \quad (\text{B4})$$

where we have used $L^{-1} \sum_k \simeq \int dk / (2\pi)$ and we have assumed zero temperature. This expression can be rewritten in terms of the optical power of the laser. The connection follows from [35]

$$\frac{P_{\text{op}}}{S} = \frac{c\epsilon_0 n}{2} E_0^2, \quad (\text{B5})$$

where S is the area of the illuminated region, c is the speed of light in vacuum, ϵ_0 is the vacuum dielectric constant, $E_0 = \omega A_0$ is the strength of the electric field, and n is the refractive index of the WSM. Then,

$$G_0^\chi \simeq \frac{e^2 v P_{\text{op}}}{8\pi \epsilon_0 n c \hbar^2 l_B^2 \omega^2 S}. \quad (\text{B6})$$

For a given laser power, we can maximize G_0^χ by making S as small as possible. Considering the diffraction limit, the minimum value of S is given by $(\lambda f)^2$, where $\lambda = 2\pi c/\omega$ is the wavelength of the light and f is a dimensionless number (the so-called f -number of the lens used to focus the light on the sample) [36]. It follows that

$$G_0^\chi \simeq \frac{e^2 v P_{\text{op}}}{32\pi^3 \epsilon_0 n c^3 \hbar^2 l_B^2 f^2} \simeq 10^{27} \frac{P_{\text{op}}[\text{W}]}{f^2} \text{cm}^{-3} \text{s}^{-1}, \quad (\text{B7})$$

where we have used $v \simeq 10^5$ m/s, $n \simeq \sqrt{30}$, and $B = 5\text{T}$. Thus, for $f \sim 1-10$, an optical power of 10–1000 mW leads to an optical generation rate of $10^{25} \text{cm}^{-3} \text{s}^{-1}$.

The preceding numerical estimate applies for a monochromatic light beam. In reality, since we are interested in a light pulse of duration dt in time, there will be a spread of frequencies of the order of $1/dt$. For each of the frequencies involved in the light beam, we can use the estimate above, with the proviso that P_{op} is the power contained in a specific frequency. The total generation rate is then obtained by integrating the rate over all relevant frequencies. We define a density of optical generation at frequency Ω ,

$$\mathcal{G}_0^\chi(\Omega) \simeq \frac{e^2 v \mathcal{P}_{\text{op}}(\Omega)}{8\pi \epsilon_0 n c \hbar^2 l_B^2 \Omega^2 S}, \quad (\text{B8})$$

such that

$$G_0^\chi = \int_{\text{gap}}^{\infty} d\Omega \mathcal{G}_0^\chi(\Omega). \quad (\text{B9})$$

In Eq. (B8), \mathcal{P}_{op} is the power density, such that $\mathcal{P}_{\text{op}}(\Omega)d\Omega$ describes the power in the frequency interval $(\Omega, \Omega + d\Omega)$. In Eq. (B9), the lower bound of the integral is equal to the optical gap (the minimum photon frequency that can induce a vertical interband transition between the $n = 0$ and $n = 1$ Landau levels). We recover the result (B6) for a monochromatic light when $\mathcal{P}_{\text{op}}(\Omega) = P_{\text{op}}\delta(\Omega - \omega)$. We can generalize this density to the case of a light pulse of duration dt via

$$\mathcal{P}_{\text{op}}(\Omega) = \frac{2dt}{\sqrt{\pi}[1 + \text{erf}(\omega dt)]} P_{\text{op}} e^{-(\Omega - \omega)^2 dt^2}, \quad (\text{B10})$$

normalized such that $\int_0^\infty \mathcal{P}_{\text{op}}(\Omega)d\Omega = P_{\text{op}}$. For an infinitely long pulse, we recover the monochromatic light beam. Then, if we still assume that $S \simeq (2\pi c f/\Omega)^2$ and if we neglect the frequency-dependence of the refractive index within a frequency range of order $1/dt$, then we obtain the following generalization of Eq. (B6):

$$G_0^\chi \simeq \frac{e^2 v P_{\text{op}}}{32\pi^3 \epsilon_0 n c^3 \hbar^2 l_B^2 f^2} \frac{2dt}{\sqrt{\pi}(1 + \text{erf}(\omega dt))} \times \int_{\text{gap}}^{\infty} e^{-(\Omega - \omega)^2 dt^2} d\Omega = \frac{e^2 v P_{\text{op}}}{32\pi^3 \epsilon_0 n c^3 \hbar^2 l_B^2 f^2} \frac{1 + \text{erf}[(\omega - \text{gap})dt]}{1 + \text{erf}(\omega dt)}. \quad (\text{B11})$$

Thus, the result of the monochromatic case is corrected by a factor

$$F = \frac{1 + \text{erf}[(\omega - \text{gap})dt]}{1 + \text{erf}(\omega dt)}. \quad (\text{B12})$$

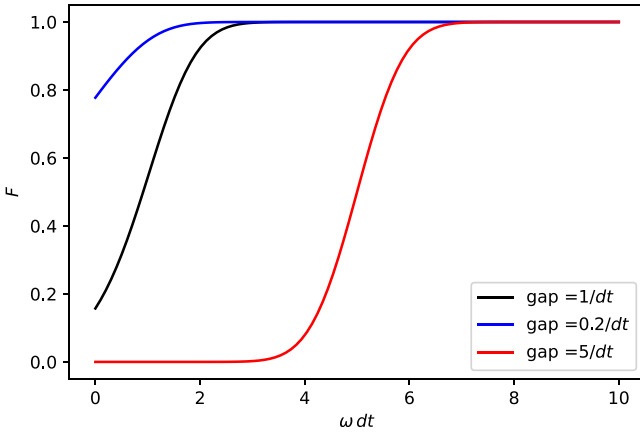


FIG. 4. Graphic representation of the function F defined in Eq. (B12).

This factor is smaller than unity (see Fig. 4), with $F \simeq 0$ when $\omega \ll 1/dt \ll \text{gap}$ and $F \rightarrow 1$ when $\omega \gg \text{gap}$. In our case of interest, where $1/dt \simeq \text{gap} \simeq \omega$, we have $F \simeq 0.5$. Thus, the estimate from the monochromatic case is not qualitatively changed.

2. Fermi golden rule estimate for the radiative recombination time

The Fermi golden rule expression for the rate of spontaneous radiative electron-hole recombination between $n = 0$ and $n = 1$ Landau levels is similar to Eq. (B2), except that we need to divide it by the number of photons impinging on the sample. Using the relation between A_0^2 and the photon number [34], we have

$$\frac{1}{\tau_r} > \frac{e^2 v \hbar}{8\pi^2 \hbar^2 l_B^2 \epsilon \omega} \simeq 10^{12} \text{ s}^{-1}, \quad (\text{B13})$$

where we have assumed $\omega \simeq v/l_B$ (typical frequency for interband transition between $n = 0$ and $n = 1$), $B = 5\text{T}$, $v = 10^5 \text{ m/s}$, and $\epsilon = 30\epsilon_0$. This estimate is a lower bound for $1/\tau_r$, as it assumes a fixed polarization of the emitted photon (the average over all polarizations will result in a multiplication by a factor of order one) and it neglects the phonon-mediated recombination. Thus, $\tau_r \lesssim 10^{-12} \text{ s}$.

APPENDIX C: LINEARIZED VAN ROOSBROECK EQUATIONS

In this Appendix, we show the details leading to Eq. (11) in the main text. First, for the $n = 1$ bands, we take a sum of the $\chi = 1$ and $\chi = -1$ equations to arrive at

$$\begin{aligned} & \mu_1(\Sigma_1 + \rho_{1,\text{eq}}^+ + \rho_{1,\text{eq}}^-) \partial_z E + \mu_1 E \partial_z \Sigma_1 + D_1 \partial_z^2 \Sigma_1 - \partial_t \Sigma_1 \\ &= \frac{\Sigma_1}{\tau_r} - \frac{1}{2}(g^+ + g^-), \end{aligned} \quad (\text{C1})$$

where E is the z component of the total electric field and $\Sigma_1 \equiv \rho_1^+ + \rho_1^- - \rho_{1,\text{eq}}^+ - \rho_{1,\text{eq}}^-$. Equation (C1) is a nonlinear differential equation. To make analytical progress, we will linearize by assuming that the departure of the carrier distribution from equilibrium is not strong. For instance, assuming that both $\rho_{1,\text{eq}}^\chi$ and Σ_1 are small (this is justified in the quantum

limit at low temperature, provided that the effect of the light in the carrier distribution is not strong), we will neglect the first term in Eq. (C1). Similarly, we approximate $\mu_1 E \partial_z \Sigma_1 \simeq \mu_1 E_0 \partial_z \Sigma_1$. Consequently, the linearized Eq. (C1) reads

$$\mu_1 E_0 \partial_z \Sigma_1 + D_1 \partial_z^2 \Sigma_1 - \partial_t \Sigma_1 \simeq \frac{\Sigma_1}{\tau_r} - \frac{1}{2}(g^+ + g^-). \quad (\text{C2})$$

Second, still for the $n = 1$ bands, we take the difference of the $\chi = 1$ and $\chi = -1$ equations to arrive at

$$\mu_1 E_0 \partial_z \Delta_1 + D_1 \partial_z^2 \Delta_1 - \partial_t \Delta_1 \simeq \frac{\Delta_1}{\tau_r} + \frac{2\Delta_1}{\tau_v} - \frac{1}{2}(g^+ - g^-), \quad (\text{C3})$$

where $\Delta_1 \equiv \rho_1^+ - \rho_1^- - \rho_{1,\text{eq}}^+ + \rho_{1,\text{eq}}^-$ and we have already performed the linearization. Note that Eq. (C3) is the same as Eq. (C2), except for the source term and the relaxation term: only $g^+ \neq g^-$ can lead to a nonzero Δ_1 and, unlike in the case of Σ_1 (as the two nodes are mirror-partners in equilibrium), elastic intervalley scattering relaxes Δ_1 . While Σ_1 is driven by $g^+ + g^-$, Δ_1 is driven by $g^+ - g^-$. Thus, in the absence of E_0 , we have no source term for Δ_1 and thus we will have $\Delta_1 = 0$ for all times and positions.

Third, we discuss the equations for $n = 0$. Equation (3) of the main text leads to

$$v \partial_z \rho_0^+ - \partial_t \rho_0^+ = \frac{\rho_0^+ - \rho_0^-}{\tau_v} - \frac{\rho_1^+ - \rho_{1,\text{eq}}^+}{\tau_r} - \frac{q^2}{4\pi^2 \hbar^2} E B_0 + \frac{g^+}{2} \quad (\text{C4})$$

$$\begin{aligned} -v \partial_z \rho_0^- - \partial_t \rho_0^- &= \frac{\rho_0^- - \rho_0^+}{\tau_v} - \frac{\rho_1^- - \rho_{1,\text{eq}}^-}{\tau_r} \\ &+ \frac{q^2}{4\pi^2 \hbar^2} E B_0 + \frac{g^-}{2}. \end{aligned} \quad (\text{C5})$$

Summing Eqs. (C4) and (C5) yields

$$v \partial_z \Delta_0 - \partial_t \Sigma_0 = -\frac{\Sigma_0}{\tau_r} + g_s, \quad (\text{C6})$$

while taking the difference between Eqs. (C4) and (C5) gives

$$v \partial_z \Sigma_0 - \partial_t \Delta_0 = 2 \frac{\Delta_0}{\tau_v} - 2 \frac{q^2}{4\pi^2 \hbar^2} E B_0 - \frac{\Delta_0}{\tau_r} + g_d. \quad (\text{C7})$$

APPENDIX D: SOLUTION OF THE VAN ROOSBROECK EQUATIONS IN FOURIER SPACE

The simplest situation in which Eq. (11) in the main text can be solved consists of an infinitely long system such that, at $z \rightarrow \pm\infty$ or $t \rightarrow \pm\infty$, the influence of the light pulse on the carrier densities is negligible. Then, we may define the Fourier transform of a function $f(z, t)$ as

$$\tilde{f}(k, \omega) = \int_{-\infty}^{\infty} dz e^{ikz} \int_{-\infty}^{\infty} dt e^{-i\omega t} f(z, t), \quad (\text{D1})$$

and use relations such as

$$\begin{aligned} & \int dt dz e^{ikz - i\omega t} \partial_z f(z, t) \\ &= \int dt dz \partial_z (e^{ikz - i\omega t} f(z, t)) \\ &- ik \int dt dz e^{ikz - i\omega t} f(z, t) = -ik \tilde{f}(k, \omega), \end{aligned} \quad (\text{D2})$$

$$\begin{aligned}
& \int dt dz e^{ikz-i\omega t} \partial_t f(z, t) \\
&= \int dt dz \partial_t (e^{ikz-i\omega t} f(z, t)) \\
&+ i\omega \int dt dz e^{ikz-i\omega t} f(z, t) = i\omega \tilde{f}(k, \omega). \quad (\text{D3})
\end{aligned}$$

Proceeding in this way, Eq. (11) of the main text can be rewritten as

$$\begin{aligned}
-ik\tilde{E}_{\text{int}} &= -\frac{q}{\epsilon}(\tilde{\Sigma}_0 + \tilde{\Sigma}_1), \\
\left(-ikv_d - D_1k^2 - i\omega - \frac{1}{\tau_r}\right)\tilde{\Sigma}_1 &= -\tilde{g}_s,
\end{aligned}$$

$$\begin{aligned}
\tilde{\Sigma}_1 &= \frac{\tilde{g}\tau_r}{1 + D_1k^2\tau_r + ikv_d\tau_r + i\omega\tau_r}, \\
\tilde{\Sigma}_0 &= \frac{\tilde{g}\tau_r(-\tau_v/\tau_a^2 - 2i\omega + \omega^2\tau_v + D_1k^2(-2 - i\omega\tau_v) + v_dk(-2i + \omega\tau_v))}{(1 + D_1k^2\tau_r + ikv_d\tau_r + i\omega\tau_r)(\tau_v/\tau_a^2 + k^2v^2\tau_v + 2i\omega - \omega^2\tau_v)}, \\
\tilde{\Delta}_0 &= \frac{\tilde{g}\tau_r\tau_v[i(1/\tau_a^2 + v^2k^2)(D_1k + iv_d) - v^2k\omega]}{v(1 + D_1k^2\tau_r + ikv_d\tau_r + i\omega\tau_r)(\tau_v/\tau_a^2 + k^2v^2\tau_v + 2i\omega - \omega^2\tau_v)} + i\frac{\epsilon\tilde{E}_{\text{light}}\omega}{qv\tau_a^2(k^2v^2 - \omega^2 + 2i\omega/\tau_v)}, \\
\tilde{E}_{\text{int}} &= -\frac{q}{\epsilon} \frac{\tilde{g}\tau_r[2v_d + i\tau_v(kv^2 + \omega v_d) + D_1k(-2i + \omega\tau_v)]}{[1 + D_1k^2\tau_r + i\tau_r(v_dk + \omega)][\tau_v/\tau_a^2 + v^2k^2\tau_v + \omega(2i - \omega\tau_v)]}. \quad (\text{D5})
\end{aligned}$$

The last term in the third line of Eq. (D5) comes from the chiral anomaly induced by the electric field of light within the chiral Landau levels. This term would be present even in the absence of light-induced interband transitions. In particular, it does not involve τ_r , because it is independent of the interband absorption rate. Note that \tilde{E}_{light} is the Fourier transform of the z component of E_{light} . If the electric field of the incident light is oriented perpendicular to the magnetic field, then the last term of the third line of Eq. (D5) will be absent. This is the situation we will adopt from now on, to distinguish the previously known physics from our new predictions.

An inverse Fourier transform of Eq. (D5),

$$f(z, t) = \int_{-\infty}^{\infty} \frac{dk}{2\pi} e^{-ikz} \int_{-\infty}^{\infty} \frac{d\omega}{2\pi} e^{i\omega t} \tilde{f}(k, \omega), \quad (\text{D6})$$

allows us to calculate the time- and space-dependence of Σ_n , Δ_n , and E_{int} .

For general light pulses, Eq. (D6) must be computed numerically. Yet, even without calculation it is obvious that Δ_0 is generally nonzero (i.e., there is a valley polarization) despite the fact that light is absorbed with equal intensity in the two valleys. The explanation for this peculiarity resides in the fact that chiral Landau levels are unidirectional, with opposite group velocities for opposite chiralities. Thus, upon light irradiation, holes in the two chiral Landau levels counterpropagate, which locally (at each z) gives rise to a nonzero Δ_0 .

Another useful result can be extracted from Eq. (D5) without any calculation, simply by observing the k -dependence of different terms and combining this with Eq. (D6). Let us neglect the term proportional to E_{light} . Then, if $E_0 = 0$ and $g(z) = g(-z)$, then we have $\Sigma_0(z) = \Sigma_0(-z)$, $\Delta_0(z) =$

$$\begin{aligned}
\left(-ikv_d - D_1k^2 - i\omega - \frac{1}{\tau_r} - \frac{2}{\tau_v}\right)\tilde{\Delta}_1 &= -\tilde{g}_d, \\
-ikv\tilde{\Delta}_0 - i\omega\tilde{\Sigma}_0 &= -\frac{\tilde{\Sigma}_1}{\tau_r} + \tilde{g}_s, \\
-ikv\tilde{\Sigma}_0 - \left(i\omega + \frac{2}{\tau_v}\right)\tilde{\Delta}_0 &= \frac{\epsilon\tilde{E}}{qv\tau_a^2} - \frac{\tilde{\Delta}_1}{\tau_r} + \tilde{g}_d, \quad (\text{D4})
\end{aligned}$$

where $\tilde{E} = \tilde{E}_{\text{light}} + \tilde{E}_{\text{int}}$. These are now algebraic equations whose solution is straightforward (though cumbersome).

For simplicity, let us first neglect the difference between g^+ and g^- (i.e., assume $g^+ \simeq g^- \equiv g$). This immediately implies $\Delta_1 = 0$, and

$-\Delta_0(-z)$, and $E_{\text{int}}(z) = -E_{\text{int}}(-z)$. This result can be understood from the facts that (i) when $E_0 = 0$ and $g(z) = g(-z)$, the system has inversion symmetry along z , and (ii) the photoexcited holes in chiral Landau levels counterpropagate, with holes of opposite chirality going opposite ways. As a result, there is an excess of holes of positive chirality on $z < 0$ and an equal excess of holes of negative chirality on $z > 0$, thereby giving rise to $\Delta_0(z) = -\Delta_0(-z)$. When $E_0 \neq 0$ or $g(z) \neq g(-z)$, inversion symmetry along z is broken, so that $\Sigma_0(z) \neq \Sigma_0(-z)$, $\Delta_0(z) \neq \Delta_0(-z)$, and $E_{\text{int}}(z) \neq -E_{\text{int}}(-z)$. The latter asymmetry in the internal electric field is crucial for the development of the transient photovoltage discussed below and also in the main text.

To gain further analytical understanding of Eq. (D5), it is useful to consider some simple limits. First, we find

$$\lim_{\tau_a \rightarrow 0} (\tilde{\Sigma}_0 + \tilde{\Sigma}_1) = 0. \quad (\text{D7})$$

This means that, at timescales that are very long compared to the dielectric relaxation time, the charge neutrality (which was initially perturbed by the fact that the photoexcited holes in the chiral Landau levels and the photoexcited electrons in the nonchiral Landau level propagate at different velocities) will be locally restored. In other words, the photoinduced holes in the chiral Landau levels and the photoinduced electrons in the nonchiral Landau level will propagate in lockstep. In the semiconductor literature, this is known as the ‘‘ambipolar transport regime’’ [29]. We note that the chiral anomaly term in the continuity equations is crucial to reach the ambipolar transport regime. Likewise, if we disregard the term proportional to E_{light} , then we find

$$\lim_{\tau_a \rightarrow 0} \tilde{\Delta}_0 = \tilde{g} \frac{(iD_1k - v_d)\tau_r}{v[1 + D_1k^2\tau_r + i\tau_r(v_dk + \omega)]}. \quad (\text{D8})$$

This result is consistent with the ambipolar transport regime: it leads to the fact that the current due to excess holes in the chiral Landau levels ($qv\Delta_0$) exactly cancels with the current from excess electrons in the nonchiral Landau level ($qv_d\Sigma_0 + qD_1\partial_z\Sigma_1$); the cancellation can be verified directly in Fourier space (k, ω). Concerning the term proportional to E_{light} in the last line of Eq. (D5), it describes an oscillatory current of intraband origin; there is no spatial charge separation (or internal electric field) associated to it, and thus is not relevant for the emergence of the ambipolar regime.

Second, a concrete situation of interest is that of a δ -function pulse in space and time, i.e., $g = g_0\delta(z)\delta(t)$ for a constant g_0 , which results in $\tilde{g} = g_0$ independent k and ω . Then, using the residue theorem,

$$\begin{aligned}\Sigma_1(z, t) &= \int_{-\infty}^{\infty} \frac{dk}{2\pi} e^{-ikz} \int_{-\infty}^{\infty} \frac{d\omega}{2\pi} e^{i\omega t} \tilde{\Sigma}_1(k, \omega) \\ &= \frac{g_0}{2\sqrt{\pi D_1 t}} e^{-(z+vd t)^2/(4D_1 t)} e^{-t/\tau_r},\end{aligned}\quad (\text{D9})$$

which agrees with the results in standard semiconductor textbooks [4]. The inverse Fourier transforms for $\tilde{\Sigma}_0$ and $\tilde{\Delta}_0$ are analytically more cumbersome. To do some reality checks, we consider the limit $(\tau_a, \tau_r, \tau_v) \rightarrow \infty$. Then, we get

$$\begin{aligned}\tilde{\Sigma}_0 &\simeq \frac{i\tilde{g}\omega}{\omega^2 - v^2k^2 - i0^+\text{sign}(\omega)}, \\ \tilde{\Delta}_0 &\simeq -\frac{i\tilde{g}vk}{\omega^2 - v^2k^2 - i0^+\text{sign}(\omega)},\end{aligned}\quad (\text{D10})$$

where $0^+ = 1/\tau_v$ is an infinitesimal positive number (kept to ensure the causality of the solution). Recalling that $\tilde{g} \propto B$, the expressions for $\tilde{\Sigma}_0$ and $\tilde{\Delta}_0$ are proportional, respectively, to the scalar and axial density response functions in the quantum limit [37]. Because the only spatial variations in our problem take place along the direction of the magnetic field (z), the relevant response functions are those with zero transverse wave vector. The axial response function appearing in the

expression for $\tilde{\Delta}_0$ is associated to the chiral anomaly [37], and its form remains unchanged at weaker magnetic fields when the system is no longer in the quantum limit.

Now let us compute the inverse Fourier transform of Eq. (D10). For δ function pulses, we obtain

$$\begin{aligned}\lim_{(\tau_a, \tau_r, \tau_v) \rightarrow \infty} \Sigma_0(z, t) &\simeq -\frac{g_0}{2} [\delta(z + vt) + \delta(z - vt)], \\ \lim_{(\tau_a, \tau_r, \tau_v) \rightarrow \infty} \Delta_0(z, t) &\simeq -\frac{g_0}{2} [\delta(z + vt) - \delta(z - vt)].\end{aligned}\quad (\text{D11})$$

For finite (τ_a, τ_r, τ_v) , this result remains relevant at timescales that are short compared to τ_a, τ_r and τ_v . In that regime, the excess holes induced optically in the chiral Landau levels counterpropagate without attenuation, with opposite group velocities for carriers of opposite chirality. The overall negative sign in the first line of Eq. (D11) is due to the fact that the optical pulse removes electrons from the chiral Landau level to put them in the nonchiral Landau levels. This explains the two lines of Eq. (D11). It is remarkable that, in this regime, the dynamics of carriers in the chiral Landau levels is decoupled from the dynamics of charge carriers in the nonchiral Landau levels. For timescales long compared to τ_a , one no longer has two decoupled and counterpropagating δ functions. Instead, as shown by Eqs. (D7) and (D8), the excess charges in the chiral Landau levels trail the excess charges in the nonchiral Landau level, to realize the ambipolar regime (local charge neutrality and zero net current due to photoinduced excess charges).

APPENDIX E: DETAILS ON THE DERIVATION OF EQ. (18) IN THE MAIN TEXT

For simplicity, we begin by assuming a Dirac δ -function light pulse in time, i.e., $\bar{g}^\pm(t) = \bar{g}_0^\pm \delta(t)$, with a constant \bar{g}_0^\pm (the ‘‘bar’’ notation has been introduced in the main text). Then, the solution of Eq. (17) in the main text with the appropriate boundary conditions is obtained by using the residue theorem,

$$\begin{aligned}\bar{\Sigma}_1 &= \Theta(t) \frac{\bar{g}_0^+ + \bar{g}_0^-}{2} e^{-t/\tau_r}, \\ \bar{\Delta}_0 &= \Theta(t) \frac{(\bar{g}_0^+ + \bar{g}_0^-)vd}{2v} \frac{\tau_d^2}{\tau_a^2} \frac{1}{(1 + \Omega^2\tau_d^2)} \left[-e^{-t/\tau_r} + e^{-t/\tau_v} \left(\cos(\Omega t) + \frac{\sin(\Omega t)}{\Omega\tau_d} \right) \right], \\ &+ \Theta(t) \frac{(\bar{g}_0^+ - \bar{g}_0^-)}{2} \frac{\tau_s^2}{\tau_a^2} \frac{1}{(1 + \Omega^2\tau_s^2)} \left\{ -\frac{\tau_a^2}{\tau_r} \left(\frac{1}{\tau_r} + \frac{2}{\tau_v} \right) e^{-t(1/\tau_r + 2/\tau_v)} + e^{-t/\tau_v} \left[-\cos(\Omega t) + \frac{\sin(\Omega t)}{\Omega\tau_s} \right] \right\},\end{aligned}\quad (\text{E1})$$

where $\Theta(t)$ is the Heaviside function, $\bar{\Delta}_0 \equiv \Delta_0 - \sigma_0 E_0 L / (qv)$, and

$$\Omega \equiv \sqrt{\frac{1}{\tau_a^2} - \frac{1}{\tau_v^2}}, \quad \frac{1}{\tau_{d(s)}} \equiv \frac{1}{\tau_v} - (+) \frac{1}{\tau_r}.\quad (\text{E2})$$

It is worth noting that Ω is the plasmon frequency in the quantum limit of a Weyl semimetal, renormalized by the damping $1/\tau_v$ [27]. Thus, we learn that $\bar{\Delta}_0$ oscillates at the plasma frequency.

In the regime in which $\tau_a \ll (\tau_r, \tau_v)$, we obtain the following approximate expression for Eq. (16) of the main text:

$$\begin{aligned}\epsilon \partial_t V_{\text{int}} &\simeq \Theta(t) qv_d \frac{(\bar{g}_0^+ + \bar{g}_0^-)}{2} e^{-t/\tau_v} \left[\cos(\Omega t) + \frac{\sin(\Omega t)}{\Omega\tau_d} \right] + \Theta(t) qv \frac{(\bar{g}_0^+ - \bar{g}_0^-)}{2} e^{-t/\tau_v} \left[-\cos(\Omega t) + \frac{\sin(\Omega t)}{\Omega\tau_s} \right] \\ &+ \Theta(t) qv_d \frac{(\bar{g}_0^+ + \bar{g}_0^-)}{2} \left(-\frac{2}{\tau_v} + \frac{1}{\tau_r} \right) \frac{\tau_a^2}{\tau_r} e^{-t/\tau_r} - \Theta(t) qv \frac{(\bar{g}_0^+ - \bar{g}_0^-)}{2} \left(\frac{2}{\tau_v} + \frac{1}{\tau_r} \right) \frac{\tau_a^2}{\tau_r} e^{-t(1/\tau_r + 2/\tau_v)}.\end{aligned}\quad (\text{E3})$$

Integrating this over time, we have

$$V_{\text{int}}(t) \simeq \begin{cases} V_{\text{int}}(\infty) + Ae^{-t/\tau_v} \sin(t/\tau_a) + Be^{-t/\tau_v} \cos(t/\tau_a) + Ce^{-t/\tau_r} + De^{-t/\tau_r - 2t/\tau_v}, & \text{for } t > 0, \\ V_{\text{int}}(0^-), & \text{for } t < 0, \end{cases} \quad (\text{E4})$$

where $V_{\text{int}}(\infty)$ and $V_{\text{int}}(0^-)$ are integration constants (corresponding to the values of V_{int} at $t \rightarrow \infty$ and $t \rightarrow 0^-$, respectively), and

$$\begin{aligned} A &= \frac{qv_d}{\epsilon} \frac{g_0^+ + g_0^-}{2} \tau_a - \frac{qv}{\epsilon} \frac{g_0^+ - g_0^-}{2} \tau_a, \\ B &= \frac{qv_d}{\epsilon} \frac{g_0^+ + g_0^-}{2} \left(-\frac{2}{\tau_v} + \frac{1}{\tau_r} \right) \tau_a^2 - \frac{qv}{\epsilon} \frac{g_0^+ - g_0^-}{2} \frac{\tau_a^2}{\tau_r}, \\ C &= \frac{qv_d}{\epsilon} \frac{g_0^+ + g_0^-}{2} \left(\frac{2}{\tau_v} - \frac{1}{\tau_r} \right) \tau_a^2, \\ D &= \frac{qv}{\epsilon} \frac{g_0^+ - g_0^-}{2} \frac{\tau_a^2}{\tau_r}. \end{aligned} \quad (\text{E5})$$

Since we are considering a δ -function pulse at $t = 0$, the influence of the pulse in $V_{\text{int}}(t)$ should vanish when $t < 0$ and $t \rightarrow \infty$. This imposes

$$V_{\text{int}}(0^-) = V_{\text{int}}(\infty) = 0. \quad (\text{E6})$$

We notice also that V_{int} is continuous at $t = 0$ ($B + C + D = 0$), as expected by integrating the left and right sides of Eq. (E3) across $t = 0$. The last two lines in Eq. (E3), which appear to be higher order in τ_a , are in fact important to obtain a solution that satisfies $V_{\text{int}}(0^+) = V_{\text{int}}(\infty) = 0$. We also notice that A is parametrically larger than B , C and D in the $\tau_a \ll (\tau_r, \tau_v)$ regime. Further assuming that τ_r is not long compared to τ_v , we can approximate

$$V_{\text{int}}(t) \simeq \frac{q}{\epsilon} \left(\frac{g_0^+ + g_0^-}{2} v_d - \frac{g_0^+ - g_0^-}{2} v \right) \tau_a e^{-t/\tau_v} \sin(t/\tau_a). \quad (\text{E7})$$

Equation (E7) was derived assuming a very short pulse in time. In practice, this would require pulses faster than τ_a , which may imply subpicosecond times for typical magnetic fields required to attain the quantum limit. For such short pulses, one might be concerned that carriers of additional nonchiral Landau levels not included in our theory could be excited significantly. Thus, if we are interested in restraining the carrier dynamics to only $n = 0$ and $n = 1$, then it is necessary to consider light pulses that are slower than τ_a . Hence, for completeness, we will consider a Gaussian light pulse with a nonzero width t , i.e.,

$$\overline{g^x}(t) = \overline{g_0^x} \frac{1}{\sqrt{2\pi} dt} e^{-t^2/(2dt^2)} \quad (\text{E8})$$

for a constant $\overline{g_0^x}$, which implies

$$\overline{g^x}(\omega) = \overline{g_0^x} e^{-\omega^2 dt^2/2}. \quad (\text{E9})$$

In the limit $dt \rightarrow 0$, we recover the results from the previous paragraphs. Let us now see how those results change when $dt \neq 0$, and possibly $dt > \tau_a$.

It turns out that the solutions for $\overline{\Sigma}_1$ and $\overline{\Delta}_0$ can still be obtained using the residue theorem to a good approximation, provided that we consider $t \gg dt$. In comparison with the solution for the δ -function pulse, the solutions for the Gaussian pulse result in the following substitutions:

$$\begin{aligned} e^{-t/\tau_r} &\rightarrow e^{-t/\tau_r} e^{dt^2/(2\tau_r^2)}, \\ e^{-t/\tau_v} &\rightarrow e^{-t/\tau_v} e^{dt^2(-1/(2\tau_a^2)+1/\tau_v^2)}, \\ \cos(\Omega t) &\rightarrow \cos[\Omega(t - dt^2/\tau_v)], \\ \sin(\Omega t) &\rightarrow \sin[\Omega(t - dt^2/\tau_v)]. \end{aligned} \quad (\text{E10})$$

Consequently, we find that the counterpart of Eq. (E7) becomes

$$\begin{aligned} V_{\text{int}}(t) &\simeq \frac{q}{\epsilon} \left(\frac{g_0^+ + g_0^-}{2} v_d - \frac{g_0^+ - g_0^-}{2} v \right) \tau_a e^{-t/\tau_v} e^{-dt^2/(2\tau_a^2)} \\ &\times \sin \left[\frac{t - dt^2/\tau_v}{\tau_a} \right], \end{aligned} \quad (\text{E11})$$

which matches with Eq. (18) of the main text for $t > dt$ (in the main text, we wrote $t - dt^2/\tau_v \simeq t$ for $t > dt$, as our regime of interest is $dt \ll \tau_v$).

APPENDIX F: WEAK MAGNETIC FIELD REGIME

In this section, we adapt our theory to the case of weak magnetic fields, where Landau quantization can be ignored. The energy spectrum is then made of two linearly dispersing Weyl cones with a constant group velocity v . The two nodes are separated from one another in momentum space. Like in the main text, we assume that the two Weyl cones are related to one another by an improper symmetry.

We denote the bands as (n, χ) , where $n = c, v$ indicates the conduction or valence band and χ labels the chirality. We assume that the Fermi level intersects the valence bands deep enough so that the thermal population of electrons in the conduction band is negligible. Moreover, we adopt the standard semiconductor convention of describing the carriers as electrons in the conduction band and holes in the valence bands (this differs from the main text, where we used the electron picture to describe the carrier dynamics in both $n = 0$ and $n = 1$ Landau levels). Thus, hereafter ρ_c^x (ρ_v^x) denotes the electron (hole) concentration in the conduction (valence) band of chirality χ .

The electric current carried by electrons in the conduction band of chirality χ can be written as

$$j_c^x = q\mu_c^x \rho_c^x E + qD_c^x \partial_z \rho_c^x, \quad (\text{F1})$$

where E is the z component of the electric field, $\mu_c^x > 0$ is the electron mobility, and $D_c^x > 0$ is the diffusion coefficient. Similarly, the electric current carried by holes in the valence

band of chirality χ can be written as

$$j_v^\chi = q\mu_v^\chi \rho_v^\chi E - qD_v^\chi \partial_z \rho_v^\chi, \quad (\text{F2})$$

where $\mu_v^\chi > 0$ is the hole mobility and $D_v^\chi > 0$ is the diffusion coefficient.

The use Eqs. (F1) and (F2) for Weyl fermions requires some comments. In a simple parabolic electronic band n , the drift current can be written as $q\mu_n \rho_n E$, where the mobility μ_n is approximately independent from the carrier concentration ρ_n . The situation changes for a linearly dispersing Weyl band. In this case, while we may insist to write the drift current as $q\mu_n^\chi \rho_n^\chi E$, the mobility can no longer be considered to be approximately independent from the carrier concentration. For example, in the absence of a magnetic field and at low temperature, the equilibrium hole concentration in the valence band can be written as

$$\rho_v^\chi = \frac{1}{6\pi^2 \hbar^3} \frac{\epsilon_F^3}{v^3}, \quad (\text{F3})$$

where $\epsilon_F > 0$ is the Fermi energy measured from the Weyl node. Under the same conditions, the mobility reads

$$\mu_v^\chi = qv^2 \tau / \epsilon_F, \quad (\text{F4})$$

where τ is the electronic lifetime. Thus, if ρ_v varies out of equilibrium due to (say) a change in ϵ_F , then so does μ_v . Concerning the diffusion coefficients D_n^χ , they are related to the conductivities $\sigma_n^\chi = q\mu_n^\chi \rho_n^\chi$ via the Einstein relation. At zero magnetic field and low temperature, we obtain $D_n^\chi \simeq v^2 \tau / 3$, which can be approximated as independent from the carrier concentration. It is with these qualifications that we write Eqs. (F1) and (F2).

Charge continuity equations now read

$$\begin{aligned} \frac{\partial j_c^\chi}{\partial z} - q \frac{\partial \rho_c^\chi}{\partial t} &= qR_c^\chi + qG_c^\chi, \\ \frac{\partial j_v^\chi}{\partial z} + q \frac{\partial \rho_v^\chi}{\partial t} &= -qR_v^\chi - qG_v^\chi - \chi \frac{q^3}{4\pi^2 \hbar^2} EB_0, \end{aligned} \quad (\text{F5})$$

where in the low temperature limit that we consider the chiral anomaly affects only the band that crosses the Fermi level (the valence band in our case), and

$$G_c^\chi = G_v^\chi = -\frac{g^\chi}{2}. \quad (\text{F6})$$

Note that the light pulse increases the number of electrons in the conduction band and the number of holes in the valence band. Concerning the relaxation rate for the excess in the charge, we have

$$\begin{aligned} R_c^\chi &= \frac{\rho_c^\chi - \rho_{c,\text{eq}}^\chi}{\tau_r} + \chi \frac{\rho_c^+ - \rho_c^-}{\tau_v}, \\ R_v^\chi &= \frac{\rho_v^\chi - \rho_{v,\text{eq}}^\chi}{\tau_r} + \chi \frac{\rho_v^+ - \rho_v^-}{\tau_v}, \end{aligned} \quad (\text{F7})$$

where $\rho_{n,\text{eq}}^\chi$ are the equilibrium densities. Like in the main text, the total charge is conserved.

Concerning Poisson's equation, it reads

$$\frac{\partial E}{\partial z} = -\frac{q}{\epsilon} \sum_{\chi=\pm 1} [(\rho_c^\chi - \rho_{c,\text{eq}}^\chi) - (\rho_v^\chi - \rho_{v,\text{eq}}^\chi)], \quad (\text{F8})$$

where we assume that, in equilibrium, the doping concentration is uniform.

Equations (F1), (F2), (F5), (F7), and (F8) form the van Roosbroeck system of equations at weak magnetic field. These equations can be linearized in the same way as in Appendix C, except for two changes. The first change comes from the fact that we must take into consideration the dependence of the mobility on the carrier concentration. For example, we write

$$\begin{aligned} \partial_z(j_n^\chi) &= q(\partial_z \mu_n^\chi) \rho_n^\chi E + q\mu_n^\chi (\partial_z \rho_n^\chi) E + q\mu_n^\chi \rho_n^\chi (\partial_z E) \\ &\quad \pm qD_n^\chi \partial_z^2 \rho_n^\chi, \end{aligned} \quad (\text{F9})$$

where the + (−) sign is for $n = c$ ($n = v$). In parabolic band systems, the first term in the right-hand side of Eq. (F9) would be omitted. In the present case, we express

$$\frac{\partial \mu_n^\chi}{\partial z} = \frac{\partial \mu_n^\chi}{\partial \rho_n^\chi} \frac{\partial \rho_n^\chi}{\partial z}. \quad (\text{F10})$$

Thus,

$$\partial_z(j_n^\chi) = q\tilde{\mu}_n(\partial_z \rho_n)E + q\mu_n \rho_n (\partial_z E), \quad (\text{F11})$$

where

$$\tilde{\mu}_n^\chi = \mu_n^\chi + \rho_n^\chi \frac{\partial \mu_n^\chi}{\partial \rho_n^\chi} \quad (\text{F12})$$

is a modified mobility. Upon linearization, we write

$$q\tilde{\mu}_n^\chi (\partial_z \rho_n)E \simeq q\tilde{\mu}_{n,\text{eq}} (\partial_z \rho_n^\chi)E_0, \quad (\text{F13})$$

where the equilibrium mobility $\tilde{\mu}_{n,\text{eq}}$ is the same for both chiralities due to the crystal symmetry relating the two Weyl cones.

The second change comes from the fact that the equilibrium hole concentration in the valence band ($\rho_{v,\text{eq}}^\chi$) is not small in our theory, and hence

$$q\mu_v \rho_{v,\text{eq}}^\chi \partial_z E \simeq q\mu_{v,\text{eq}} \rho_{v,\text{eq}}^\chi \partial_z E_{\text{int}} \quad (\text{F14})$$

will not be neglected.

Therefore, the linearization of van Roosbroeck's equations yields

$$\begin{aligned} \partial_z E_{\text{int}} &= -\frac{q}{\epsilon} (\Sigma_c - \Sigma_v), \\ \left(\tilde{\mu}_{c,\text{eq}} E_0 \partial_z + D_c \partial_z^2 - \partial_t - \frac{1}{\tau_r} \right) \Sigma_c &= -g_s, \\ \left(\tilde{\mu}_{c,\text{eq}} E_0 \partial_z + D_c \partial_z^2 - \partial_t - \frac{1}{\tau_r} - \frac{2}{\tau_v} \right) \Delta_c &= -g_d, \\ (-\tilde{\mu}_{v,\text{eq}} E_0 \partial_z + D_v \partial_z^2 - \partial_t) \Sigma_v &= -g_s + \frac{1}{\tau_r} \Sigma_c + \mu_{v,\text{eq}} (\rho_{v,\text{eq}}^+ + \rho_{v,\text{eq}}^-) \partial_z E_{\text{int}}, \\ \left(-\tilde{\mu}_{v,\text{eq}} E_0 \partial_z + D_v \partial_z^2 - \partial_t - \frac{2}{\tau_v} \right) \Delta_v &= -g_d + \frac{1}{\tau_r} \Delta_c + \frac{q^2}{2\pi^2 \hbar^2} EB_0, \end{aligned} \quad (\text{F15})$$

where $\Sigma_n \equiv \sum_\chi (\rho_n^\chi - \rho_{n,\text{eq}}^\chi)$ and $\Delta_n \equiv \sum_\chi \chi (\rho_n^\chi - \rho_{n,\text{eq}}^\chi)$.

Now, let us study the transient photovoltage using the same approach as in the strong field regime. We consider the

situation where a Weyl semimetal film of length L along the z direction is placed between two contacts and subjected to a light pulse centered at time $t = 0$. The light pulse acts far enough from the contacts, such that carrier densities at $z = \pm L/2$ remain at their equilibrium values. In this condition, Eqs. (F15) can be solved in Fourier space, like in Appendix C. As a result, the following relation is verified for the particle photocurrent:

$$\delta j = -qv_c \Sigma_c + qv_v \Sigma_v + q\mu_{v,\text{eq}} (\rho_{v,\text{eq}}^+ + \rho_{v,\text{eq}}^-) E_{\text{int}} + qD_c \partial_z \Sigma_c - qD_v \partial_z \Sigma_v = -\epsilon \partial_t E_{\text{int}}, \quad (\text{F16})$$

where $v_c = -\tilde{\mu}_{c,\text{eq}} E_0$ is the drift velocity of electrons in the conduction band and $v_v = \tilde{\mu}_{v,\text{eq}} E_0$ is the drift velocity of holes in the valence band. Integrating Eq. (F16) over the sample length and applying the boundary conditions, we obtain

$$\epsilon \partial_t V_{\text{int}} = \overline{\delta j} = -qv_c \overline{\Sigma_c} + qv_v \overline{\Sigma_v} - q\mu_{v,\text{eq}} (\rho_{v,\text{eq}}^+ + \rho_{v,\text{eq}}^-) V_{\text{int}}, \quad (\text{F17})$$

where $\overline{\Sigma_c}$ and $\overline{\Sigma_v}$ obey, according to the spatial integration of Eq. (F15),

$$\left(\partial_t + \frac{1}{\tau_r} \right) \overline{\Sigma_c} = \overline{g_s}, \quad (\text{F18a})$$

$$\partial_t \overline{\Sigma_v} = \overline{g_s} - \frac{1}{\tau_r} \overline{\Sigma_c}. \quad (\text{F18b})$$

Considering a δ -function light centered at $t = 0$, i.e., $\overline{g_s} = \overline{g_0} \delta(t)$, Eq. (F18) gives

$$\overline{\Sigma_c} = \overline{\Sigma_v} = \overline{g_0} e^{-t/\tau_r} \Theta(t), \quad (\text{F19})$$

where $\Theta(t)$ is the step function. The fact that $\overline{\Sigma_c} = \overline{\Sigma_v}$ can also be obtained from integration of Poisson's equation with the boundary condition that E_{int} is negligible at the contacts.

Consequently, Eq. (F17) becomes

$$\partial_t V_{\text{int}} = \frac{q}{\epsilon} \overline{g_0} (v_v - v_c) e^{-t/\tau_r} \Theta(t) - \frac{\sigma_v}{\epsilon} V_{\text{int}}, \quad (\text{F20})$$

where $\sigma_v = q\mu_{v,\text{eq}} (\rho_{v,\text{eq}}^+ + \rho_{v,\text{eq}}^-)$ is the equilibrium conductivity at low temperature and $\epsilon/\sigma_v \equiv \tau_D$ is the dielectric relaxation time for excess charge in the valence band. Integrating over time, using $V_{\text{int}}(t < 0) = 0$ and imposing the continuity of V_{int} at $t = 0$, we arrive at

$$V_{\text{int}}(t) = \frac{q}{\epsilon} \overline{g_0} (v_v - v_c) \frac{\tau_D \tau_r}{\tau_D - \tau_r} (e^{-t/\tau_D} - e^{-t/\tau_r}). \quad (\text{F21})$$

The fact that photoexcited electrons and holes drift in opposite directions under the action of E_0 (i.e., $v_c v_v < 0$) is crucial for the development of the transient photovoltage. Some limiting regimes of Eq. (F21) are

$$V_{\text{int}}(t) \simeq \frac{q}{\epsilon} \overline{g_0} (v_v - v_c) \tau_D e^{-t/\tau_r}, \quad \text{for } \tau_D \ll \tau_r,$$

$$V_{\text{int}}(t) \simeq \frac{q}{\epsilon} \overline{g_0} (v_v - v_c) \tau_r e^{-t/\tau_D}, \quad \text{for } \tau_D \gg \tau_r. \quad (\text{F22})$$

In sum, the transient photovoltage at weak magnetic fields decays in a nonoscillatory fashion. This behavior differs qualitatively from the strong magnetic field regime (see main text), where V_{int} oscillates at the plasma frequency due to the chiral anomaly term in the van Roosbroeck equations. At weak fields, the chiral anomaly term in Eq. (F7) does not enter in the transient photovoltage. Nevertheless, the chiral anomaly influences V_{int} indirectly, through its participation in the drift velocities. It is well-known that, at weak field, chiral anomaly causes an anisotropy of order B_0^2 in the conductivity tensor [38]. Since the drift velocity scales with the conductivity, it is different (by an amount of order B_0^2) when the magnetic field is parallel or perpendicular to the applied electric field. Thus, the much-studied anisotropic magnetoresistance of Weyl semimetals finds a counterpart in the transient photovoltage under a pulsed light.

-
- [1] W. Van Roosbroeck, *Bell Syst. Tech. J.* **29**, 560 (1950).
[2] A. de Mari, *Solid-State Electron.* **11**, 1021 (1968).
[3] C. G. Fonstad, *Microelectronic Devices and Circuits* (McGraw-Hill College, New York, NY, 1994).
[4] J. P. McKelvey, *Solid State and Semiconductor Physics* (Robert E. Krieger Publishing Company, Malabar, FL, 1984).
[5] S. Selberherr, *Analysis and Simulation of Semiconductor Devices* (Springer, New York, NY, 1984).
[6] P. Farrell, N. Rotundo, D. H. Doan, M. Kantner, J. Fuhrmann, and T. Koprucki, Numerical Methods for Drift-diffusion Models, Tech. Rep. (Weierstraß-Institut für Angewandte Analysis und Stochastik, Berlin, 2016).
[7] S. M. Sze, Y. Li, and K. K. Ng, *Physics of Semiconductor Devices* (John Wiley & Sons, New York, NY, 2021).
[8] See e.g., the *Semiconductor Module User's Guide*, COMSOL Multiphysics® (COMSOL AB, Stockholm, Sweden, 2018).
[9] M. Vergniory, L. Elcoro, C. Felser, N. Regnault, B. A. Bernevig, and Z. Wang, *Nature (London)* **566**, 480 (2019).
[10] B. J. Wieder, B. Bradlyn, J. Cano, Z. Wang, M. G. Vergniory, L. Elcoro, A. A. Soluyanov, C. Felser, T. Neupert, N. Regnault *et al.*, *Nat. Rev. Mater.* **7**, 196 (2022).
[11] M. G. Vergniory, B. J. Wieder, L. Elcoro, S. S. Parkin, C. Felser, B. A. Bernevig, and N. Regnault, *Science* **376**, eabg9094 (2022).
[12] J. Liu, F. Xia, D. Xiao, F. J. Garcia de Abajo, and D. Sun, *Nat. Mater.* **19**, 830 (2020).
[13] M. J. Gilbert, *Commun. Phys.* **4**, 70 (2021).
[14] S. A. Parameswaran, T. Grover, D. A. Abanin, D. A. Pesin, and A. Vishwanath, *Phys. Rev. X* **4**, 031035 (2014).
[15] N. P. Armitage, E. J. Mele, and A. Vishwanath, *Rev. Mod. Phys.* **90**, 015001 (2018).
[16] C. P. Weber, *J. Appl. Phys.* **129**, 070901 (2021).
[17] C. Bao, P. Tang, D. Sun, and S. Zhou, *Nat. Rev. Phys.* **4**, 33 (2022).
[18] L. E. Golub and E. L. Ivchenko, *Phys. Rev. B* **98**, 075305 (2018).
[19] J. Ahn, G.-Y. Guo, and N. Nagaosa, *Phys. Rev. X* **10**, 041041 (2020).
[20] Q. Ma, A. G. Grushin, and K. S. Burch, *Nat. Mater.* **20**, 1601 (2021).
[21] M. M. Jadidi, M. Kargarian, M. Mittendorff, Y. Aytac, B. Shen, J. C. König-Otto, S. Winnerl, N. Ni, A. L. Gaeta,

- T. E. Murphy, and H. D. Drew, *Phys. Rev. B* **102**, 245123 (2020).
- [22] A. L. Levy, A. B. Sushkov, F. Liu, B. Shen, N. Ni, H. D. Drew, and G. S. Jenkins, *Phys. Rev. B* **101**, 125102 (2020).
- [23] B. Cheng, T. Schumann, S. Stemmer, and N. P. Armitage, *Sci. Adv.* **7**, eabg0914 (2021).
- [24] A. Burkov, *J. Phys.: Condens. Matter* **27**, 113201 (2015).
- [25] R. Ilan, A. G. Grushin, and D. I. Pikulin, *Nat. Rev. Phys.* **2**, 29 (2020).
- [26] M. Massicotte, G. Soavi, A. Principi, and K.-J. Tielrooij, *Nanoscale* **13**, 8376 (2021).
- [27] J.-M. Parent, R. Côté, and I. Garate, *Phys. Rev. B* **102**, 245126 (2020).
- [28] S. A. Hawks, B. Y. Finck, and B. J. Schwartz, *Phys. Rev. Appl.* **3**, 044014 (2015).
- [29] J. G. Champlain, *Appl. Phys. Lett.* **99**, 123502 (2011).
- [30] M. Mattheakis, G. P. Tsironis, and E. Kaxiras, in *Nanoplasmonics: Fundamentals and Applications*, edited by G. Barbillon (IntechOpen, 2017), Chap. 1.
- [31] R. Kersting, K. Unterrainer, G. Strasser, H. F. Kauffmann, and E. Gornik, *Phys. Rev. Lett.* **79**, 3038 (1997).
- [32] R. Kersting, J. N. Heyman, G. Strasser, and K. Unterrainer, *Phys. Rev. B* **58**, 4553 (1998).
- [33] J. N. Heyman, P. Neocleous, D. Hebert, P. A. Crowell, T. Müller, and K. Unterrainer, *Phys. Rev. B* **64**, 085202 (2001).
- [34] B. K. Ridley, *Quantum Processes in Semiconductors* (Oxford University Press, Oxford, UK, 2013).
- [35] D. Griffiths, *Introduction to Electrodynamics* (Pearson Education, London, UK, 2014).
- [36] A. Siegman, *Lasers* (University Science Books, Melville, NY, 1986).
- [37] P. Rinkel, P. L. S. Lopes, and I. Garate, *Phys. Rev. B* **99**, 144301 (2019).
- [38] D. T. Son and B. Z. Spivak, *Phys. Rev. B* **88**, 104412 (2013).